

Low-Temperature Thermodynamic Properties of Vanadium. II. Mixed State*†

RAY RADEBAUGH‡ AND P. H. KEESOM

Department of Physics, Purdue University, Lafayette, Indiana

(Received 8 March 1966)

The specific heat of a single-crystal vanadium sample (resistivity ratio=140) has been measured in 12 different magnetic fields between 0.5 and 5.4°K to study the mixed state. The specific heat above approximately H_c is found to be independent of sample history, which leads to a complete thermodynamic description of the mixed state. The upper critical field $H_{c2}(t)$ is found from the specific heat at high fields and from heating and cooling curves at low fields and is used with $H_{c1}(t)$ determined from specific-heat measurements in part I of this investigation to obtain the parameter $\kappa_1(t) = H_{c2}(t)/\sqrt{2}H_c(t)$. The Ginzburg-Landau parameter $\kappa \equiv \kappa_1(1)$ is found to be 0.979 ± 0.010 for this sample and, when extrapolated to infinite electron mean free path, yields the value $\kappa_0 = 0.848 \pm 0.015 > 1/\sqrt{2}$, which proves that vanadium, like niobium, is an intrinsic type-II superconductor. The behavior of $\kappa_1(t)/\kappa$ for vanadium is shown to be nearly identical to that for niobium and is higher at all temperatures than the theoretical prediction of Gor'kov. In particular $\kappa_1(0)/\kappa$ is 1.50 ± 0.02 compared with the theoretical value 1.25, which points out the need for a refinement of the theory concerning intrinsic type-II superconductors. Magnetization curves are thermodynamically deduced from the specific-heat data and are used to find $H_{c1}(t)$, given by $1150(1-t^2)$ Oe. In addition the curves appear to represent the average behavior of actual magnetization measurements in increasing and decreasing fields. The parameter $\kappa_2(t)$ calculated from the slopes of the deduced magnetization curves is in excellent agreement near $t=1$ with the prediction of Maki and Tsuzuki, and at low temperatures approaches the value $\kappa_2(0)/\kappa = 2.66$. A reliable estimate of the Fermi-surface area, given by $S/S_f = 0.714$, is obtained from the value of κ_0 , which then leads to the values $\lambda_L(0) = 398 \text{ \AA}$, $\xi_0 = 450 \text{ \AA}$, and $l = 2450 \text{ \AA}$.

I. INTRODUCTION

USING the Ginzburg-Landau theory,¹ Abrikosov² showed that in the case when the surface energy between superconducting and normal regions is negative, magnetic flux starts to penetrate the material at a lower critical field H_{c1} , and this process will be completed when the upper critical field H_{c2} is reached. The magnetization of such a material is shown in Fig. 1. Materials exhibiting this type of behavior are known as type-II superconductors. By way of comparison, the magnetization of a type-I superconductor drops abruptly to zero at the thermodynamic critical field H_c , also shown in Fig. 1. The critical fields of a superconductor vary with temperature in a manner shown in Fig. 2. The mixed state of a type-II superconductor is that region between H_{c1} and H_{c2} and is entirely different from the intermediate state of a type-I superconductor. In Abrikosov's model the mixed state exists even with the field parallel to an infinitely long cylinder and is comprised of a lattice of quantized, flux-enclosing, supercurrent vortices, in agreement with experiment.³ The intermediate state of type-I superconductors, on the other hand, consists of macroscopic laminae of

superconducting and normal regions and exists only when the demagnetizing factor is not zero. Type-II superconductivity occurs when the parameter $\kappa_1(t)$, defined by

$$\kappa_1(t) = H_{c2}(t)/\sqrt{2}H_c(t), \quad t = T/T_c, \quad (1)$$

is greater than $1/\sqrt{2} = 0.707$. The Ginzburg-Landau parameter κ is taken as $\kappa_1(1)$, which is always the minimum value of $\kappa_1(t)$, except for paramagnetically limited superconductors.

A considerable amount of experimental work has been done in the last few years on the properties of type-II superconductors after they were first described by Abrikosov. Most of the work, however, has been done on alloys which have very short electronic mean free paths, and the results, in general, agree very well qualitatively with the predictions of the Ginzburg-Landau-Abrikosov-

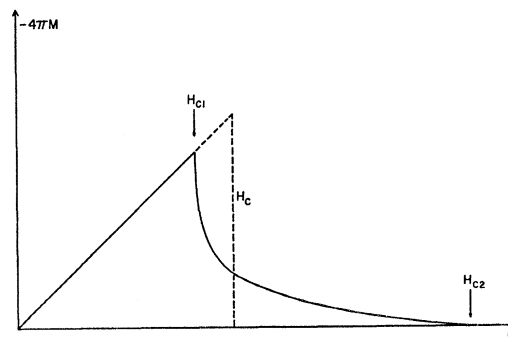


FIG. 1. Magnetization of a type-II superconductor (solid line) compared with that of a type-I superconductor (dashed line).

* Work supported by Advanced Research Projects Agency and U. S. Army Research Office (Durham).

† Preliminary reports of this work were given at the meeting of the American Physical Society, March, 1965 [Bull. Am. Phys. Soc. **10**, 358 (1965)].

‡ Present address: Institute for Materials Research, National Bureau of Standards, Boulder, Colorado.

¹ V. L. Ginzburg and L. D. Landau, Zh. Eksperim. i Teor. Fiz. **20**, 1064 (1950).

² A. A. Abrikosov, Zh. Eksperim. i Teor. Fiz. **32**, 1442 (1957) [English transl.: Soviet Phys.—JETP **5**, 1174 (1957)].

³ D. Cribier, B. Jacrot, L. Madhav Rao, and B. Farnoux, Phys. Letters **9**, 106 (1964).

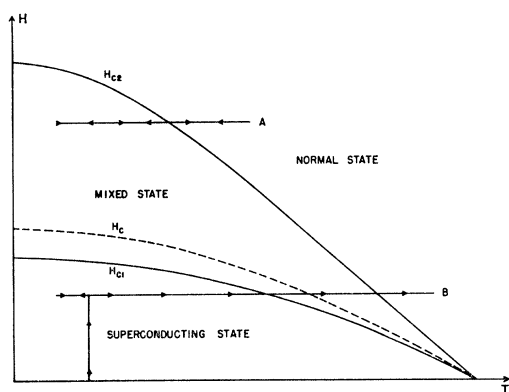


FIG. 2. The three states and the critical field curves of a type-II superconductor. The paths A and B indicate different sample histories used in the measurements of specific heat.

Gor'kov (GLAG) theory.^{1,2,4} Quantitative agreement, though, does not always occur.

As the mean free path is increased, κ decreases and approaches a value κ_0 , which is less than $1/\sqrt{2}$ for nearly all of the superconducting elements. Niobium is a rare exception⁵ with $\kappa_0=0.76$.⁶ Experiments on high-purity niobium⁷⁻⁹ indicate a somewhat different behavior from that of alloys and also from that of pure compounds, which have rather high values of κ_0 . Theoretical predictions based on the GLAG theory and applicable to pure metals do not give a good quantitative description of the behavior of niobium.

It is of interest to see if the behavior of niobium is characteristic of the material itself or of intrinsic, low- κ type-II superconductors in general. This question could only be answered if another intrinsic, low- κ type-II superconductor existed. Tantalum, which at first showed promise, turned out to be an intrinsic, type-I superconductor.¹⁰ All experiments on vanadium have indicated type-II behavior, but most of the samples studied were of quite low purity. Vanadium is extremely difficult to purify, but we have been fortunate in obtaining a rather pure sample (resistance ratio=140) from the Ford Scientific Laboratory. This sample displayed type-II superconductivity,¹¹ and this paper shows that $\kappa_0=0.848$, indicating that vanadium is indeed an intrinsic, low- κ type-II superconductor. Just recently Martin and Rose-

Innes¹² suggested the value $\kappa_0 \approx 1.7$ from their magnetic measurements on a much less pure sample without performing an extrapolation of κ to infinite mean free path. This paper will present the results of specific-heat measurements on the mixed state of vanadium and show that they completely describe the mixed state thermodynamically in addition to defining the boundaries $H_{c1}(T)$ and $H_{c2}(T)$. Results of a few magnetization measurements will also be given and compared with the magnetization thermodynamically deduced from the specific heat. It will be shown that vanadium behaves almost identically to niobium in every respect. Therefore, the behavior of both vanadium and niobium suggests a need for a refinement of the GLAG theory and its extensions to lower temperatures for intrinsic low κ type-II superconductors.

II. EXPERIMENTAL DETAILS

A. Specific-Heat Measurements

The experimental techniques used in measuring the specific heat of the mixed state are nearly identical to those already described¹³ for the superconducting and normal states. The magnetic field necessary for making measurements of the mixed state was produced by an 8-cm-i.d. superconducting magnet of copper-plated Nb-25% Zr wire. The field produced by the magnet was homogeneous within $\pm 0.2\%$ over the sample length. The magnetic field was determined by measuring the current through the magnet and multiplying by a factor based on the coil geometry and number of windings. An effect on the field due to the presence of the superconducting wire was neglected. Measurements by Maxfield and Merrill¹⁴ indicate that this effect should be less than 0.1% in the case of our magnet. In a separate experiment the field was measured with a Hall probe at 50 and 100 Oe and the results agreed with the calculated values to within experimental error (1%). A superconducting short was connected to the magnet to permit operation in the persistent mode. Even with the short heated into the normal state, the time constant of the magnet and short was quite long, which made it necessary to wait about 5 min. for equilibrium before transferring the magnet into the persistent mode. This fact was not realized in the preliminary measurements reported earlier¹¹ and gave rise to a large error in the reported magnetic field. Operating a superconducting magnet in the persistent mode has the disadvantage that the total flux passing through the magnet remains constant. As a result, the applied field H changes as the susceptibility of the sample changes. However, in this experiment the sample diameter is only 0.7 cm compared

⁴ L. P. Gor'kov, Zh. Eksperim. i Teor. Fiz. **36**, 1918 (1959) [English transl.: Soviet Phys.—JETP **9**, 1364 (1959)].

⁵ T. F. Stromberg and C. A. Swenson, Phys. Rev. Letters **9**, 370 (1962).

⁶ T. F. Stromberg and C. A. Swenson, Bull. Am. Phys. Soc. **10**, 358 (1965); T. F. Stromberg, Ph.D. thesis, Department of Physics, Iowa State University, Ames, Iowa, 1965 (unpublished).

⁷ T. McConville and B. Serin, Phys. Rev. **140**, A1169 (1965).

⁸ A. R. Strnad and Y. B. Kim, in *Proceedings of Symposium on Quantum Fluids, University of Sussex, 1965* (North-Holland Publishing Company, Amsterdam, to be published).

⁹ T. Ohtsuka, Phys. Letters **17**, 194 (1965).

¹⁰ J. I. Budnick, Phys. Rev. **119**, 1578 (1960); J. Buchanan, G. K. Chang, and B. Serin, J. Phys. Chem. Solids **26**, 1183 (1965).

¹¹ P. H. Keesom and Ray Radebaugh, Phys. Rev. Letters **13**, 685 (1964).

¹² R. B. Martin and A. C. Rose-Innes, Phys. Letters **19**, 467 (1965).

¹³ Ray Radebaugh and P. H. Keesom, preceding paper, Phys. Rev. **149**, 209 (1966).

¹⁴ B. W. Maxfield and J. R. Merrill, Rev. Sci. Instr. **36**, 1083 (1965).

with 8 cm for the magnet i.d.; thus, the applied field changes by only 0.8% when the sample goes from the superconducting state to the normal state. All data for $H_{c2}(T)$ were obtained by applying the magnetic field while the sample was in the normal state.

The specific-heat measurements are made by changing the temperature in a constant field. The measurements of the mixed state are conveniently divided into two categories: $H > H_{c1}(0)$ and $H < H_{c1}(0)$ (see Fig. 2). (For this sample $H_{c1}(0) = 1150$ Oe). For $H > H_{c1}(0)$ the material remains in the mixed state at $T = 0^\circ\text{K}$ and must undergo a phase transition at H_{c2} , whereas for $H < H_{c1}(0)$ the material exists in the superconducting state for sufficiently low temperatures and experiences phase transitions at both H_{c1} and H_{c2} . It will be shown later that the specific heat in the mixed state above approximately H_c is independent of sample history. Hake and Brammer¹⁵ measured the specific heat of V-5 at.% Ta in the mixed state and also found the specific heat to be independent of sample history. However, it will be seen that the specific heat below about H_c is highly dependent on the sample history, and so it is important to specify the exact path used to establish the sample state. For the set of measurements with $H > H_{c1}(0)$ the field was applied before cooling, as represented by path *A* in Fig. 2, since this was faster than other paths. For $H < H_{c1}(0)$, however, the field was applied after most of the cooling took place, as represented by path *B*, to eliminate flux trapping when cooling through H_{c1} . For unknown reasons it was very difficult to keep the sample temperature from rising up to about 1°K while applying the field in the superconducting state, even if the field was increased as slowly as 3 Oe min^{-1} , and so path *B* shows that some cooling was done after the field was applied. In order to observe the effect of flux trapping and of sample history, one set of measurements with $H < H_{c1}(0)$ was also made with the field applied before cooling.

Heating and cooling curves were taken to determine the transition temperature very precisely for fields of 2000 Oe and less. A heating or cooling rate of about $0.02 \text{ deg min}^{-1}$ was used, which gave approximately a 45° slope on the recorder chart. Above 2000 Oe the transition was too broad and the change in temperature drift was too small to determine the transition temperature by this method.

B. Magnetization Measurements

Magnetization measurements were done ballistically with a detector coil sampling the central portion of the same cylindrical sample as used in the specific heat measurements. The galvanometer sensitivity of $\pm 1 \text{ G}$ was the limiting factor in the precision of the data. The same low field Nb-25% Zr solenoid described previously for the specific-heat measurements was used to apply the

magnetic field. Three methods of measuring the magnetization were employed. In the first method the sample was moved rapidly from one 170-turn coil to a second identical but oppositely wound coil 10 cm away. The two coils were situated symmetrically with respect to the transverse solenoid center line. The magnetic field at the two coils was 3.7% less than the field at the center of the solenoid; thus, the sample was subjected to a slight field fluctuation in going from one coil to the other. In the second method a stationary sample and a moving coil were used to eliminate the need for a fluctuating magnetic field on the sample. Results obtained with this method were essentially the same as with the first method. Finally, in the third method both sample and coil remained stationary, and a galvanometer deflection was produced by rapidly heating the sample into the normal state.¹⁶ However, this procedure has the disadvantage of destroying the sample history, and so for each measurement the sample state and its history had to be established again. A lead cylinder of the same size as the vanadium sample was initially used to calibrate the apparatus. The perfect diamagnetic region of the vanadium sample was used for calibration in subsequent measurements.

C. Errors

The systematic errors in the specific heat due to inaccuracies in the temperature scale, addenda corrections, heater resistance, current, and timing errors should not exceed 2% at the lowest and highest temperatures and should decrease to about 1% between 1 and 4.2°K . The accuracy of the magnetic field is limited by the uncertainty in the factor relating the field and the current. It is estimated that the magnetic field is accurate to about 0.5%. Magnetization measurements are probably accurate to about 1%. Unless otherwise stated, error limits given for experimental quantities are those found from the random scatter of the data and represent the standard deviation for that quantity.

D. Sample

The single crystal vanadium sample was the same as that used in the study of the superconducting and normal states.¹³ The cylindrical sample was 7 mm in diameter by 19 mm long and contained 0.08529 moles. The axis of the cylinder was along the $\langle 110 \rangle$ direction. The demagnetizing factor for a cylinder with these dimensions is 0.092 at the center,¹⁷ but this is, by no means, uniform throughout the sample. The sample had a resistance ratio R_{295}/R_0 of 140 measured potentiometrically. A field of about 2600 Oe was used to quench superconductivity for measuring R_0 at 4.2°K .

¹⁶ S. H. Goedemoed, A. van der Giessen, D. de Klerk, and C. J. Gorter, *Phys. Letters* **3**, 250 (1963).

¹⁷ *American Institute of Physics Handbook* (McGraw-Hill Book Company, Inc., New York, 1963), 2nd ed., Chap. 5, p. 237.

¹⁵ R. R. Hake and W. G. Brammer, *Phys. Rev.* **133**, A719 (1964).

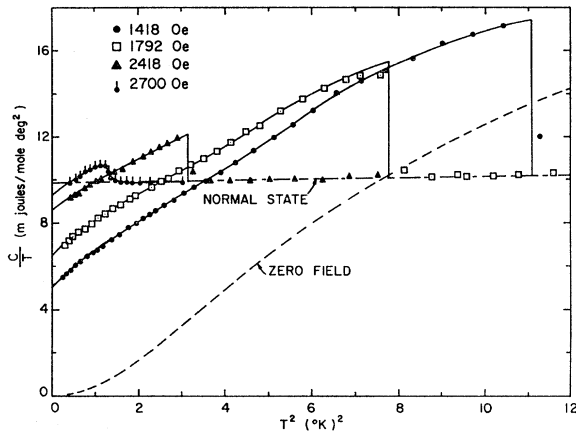


FIG. 3. Specific heat of vanadium in the mixed state for fields greater than $H_{c1}(0)$. In each case the magnetic field was applied before cooling.

III. RESULTS AND DISCUSSION

A. Specific Heat for H Greater than $H_{c1}(0)$

Figure 3 shows the specific heat in four different magnetic fields which are greater than $H_{c1}(0)$ and which cause the sample to remain in the mixed state even at $T=0^\circ\text{K}$. Data obtained in fields of 1996 and 2841 Oe show similar behavior but, for the sake of clarity, are not shown in this figure. The intercepts for each curve indicate that the specific heat in the mixed state contains a linear term, $\gamma_m T$, where γ_m increases with magnetic field. The appearance of the linear term can be a result of a certain fraction of the material in the mixed state behaving as if normal-like, which agrees with a proposal by Rosenblum and Cardona.¹⁸ This behavior follows from calculations by Caroli *et al.*,¹⁹ who showed that excitations with a very small energy gap exist within a coherence distance of an Abrikosov flux line. This energy gap is on the order of Δ_∞^2/E_F , where Δ_∞ is the energy gap in zero field and E_F is the Fermi energy. For vanadium, which has a relatively small Fermi

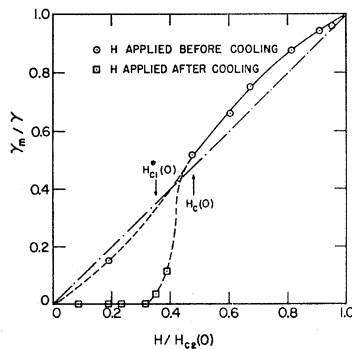


FIG. 4. The ratio of the linear term in specific heat to that of the normal state as a function of the applied field. The term $H_{c1}^*(0) = H_{c1}(0)(1-n)$ is the applied field necessary to produce the field $H_{c1}(0)$ in the sample with demagnetizing factor $n=0.092$.

¹⁸ B. Rosenblum and M. Cardona, Phys. Rev. Letters **12**, 657 (1964).

¹⁹ C. Caroli, P. G. de Gennes, and J. Matricon, Phys. Letters **9**, 307 (1964); C. Caroli and J. Matricon, Phys. Kondensierten Materie **3**, 380 (1965).

energy of about 1 eV, this gap corresponds to a temperature of about 10^{-2}°K . Using microwave surface-resistance measurements, Rosenblum and Cardona showed that the normal-like regions should occupy a fraction $H/H_{c2}(T)$ of the material. In the present investigation the ratio of γ_m to γ determines the fraction of the material existing in the normal-like state at $T=0^\circ\text{K}$. This fraction is shown in Fig. 4. In this figure $H_{c1}^* = H_{c1}(1-n)$ is the applied field which produces the field $H_{c1}(0)$ in the sample with demagnetizing factor of $n=0.092$. The region below $H_{c1}(0)$ will be discussed in the next section. The results indicate a maximum deviation in the mixed state of about 10% from the simple relationship $H/H_{c2}(0)$. The demagnetizing factor of 0.092 produces only a slight correction to H , ranging from 0 at H_{c2} to about 3% just above H_{c1} , not nearly enough to give agreement with the line $H/H_{c2}(0)$. Marcus²⁰ has given another explanation for the linear term in the specific heat by showing that it arises from a proper change of the order parameter with temperature. The values of γ_m/γ calculated by Marcus are a few percent larger than $H/H_{c2}(0)$ and in excellent agreement with experiment. However, our results do not permit us to distinguish between the two possible explanations for the linear term. A simple relationship for the fraction γ_m/γ is obtained when this is plotted against t_H^2 , as in Fig. 5, where t_H is the reduced temperature of the transition from mixed to normal state in the applied field H . From this figure it follows that $\gamma_m/\gamma = 1 - 1.24t_H^2$ in the mixed state.

The transition from the mixed state to the normal state gives no indication of latent heat, and so this transition is of second order or higher. However, in order to simplify the mathematical description, we shall consider the transition as being strictly second order, which is not inconsistent with our measurements. For low fields the total transition width is only about 1 mdeg, as determined from heating and cooling curves. At the very high fields the transition tends to broaden out (see the measurements in 2700 Oe), though most of this

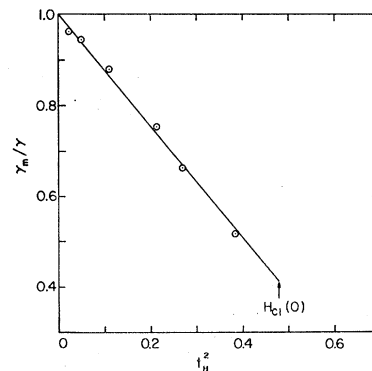
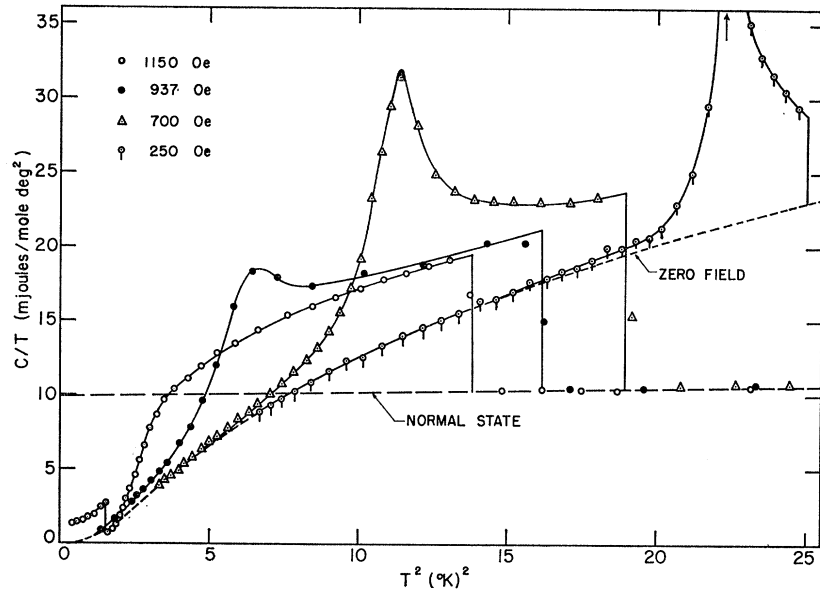


FIG. 5. The ratio of the mixed-state linear term in specific heat to that of the normal state as a function of the reduced temperature of the transition from the mixed to normal state in the field H .

²⁰ P. M. Marcus, Conference on the Physics of Type-II Superconductors, Cleveland, 1964 (unpublished); in *Proceedings of the IX International Conference on Low Temperature Physics, Columbus, Ohio, 1964* (Plenum Press, Inc., New York, 1965), p. 550.

FIG. 6. Specific heat of vanadium in fields less than $H_{c1}(0)$. In each case the field was applied after cooling. The maximum C/T in the field of 250 Oe is about $47 \text{ mJ mole}^{-1} \text{ deg}^{-2}$.



broadening can be attributed to the inhomogeneity of the applied field. Since no latent heat is present at the transition, the entropies of the mixed and normal states must agree at the transition. Entropy calculations from specific-heat data show that in all fields with $H > H_{c1}(0)$ the entropies of the mixed and normal states agree at the transition to within 0.5% or better. This proves that irreversible heating effects are not present in the mixed state except, perhaps, in the region very near H_{c1} , since no data were obtained with fields in the range between $H_{c1}(0)$ and $H_c(0)$.

B. Specific Heat for H Less than $H_{c1}(0)$

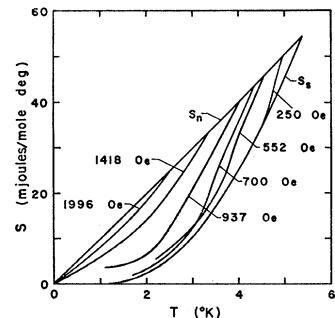
The specific heat in fields less than $H_{c1}(0)$ is shown in Fig. 6. In each case the sample was cooled in zero field to eliminate trapped flux in the superconducting state. As the figure shows, the specific heat coincides with the zero-field specific heat for sufficiently low temperatures with the exception of the case of $H = 1150$ Oe, which will be discussed separately later. As the temperature is increased, the specific heat at first gradually rises above the zero-field value and finally rises rapidly to a peak. McConville and Serin²¹ observed this peak in the specific heat of niobium and attributed it to flux penetration, which causes a change from the superconducting state to the mixed state. In this figure it can be seen that for low fields the peak for vanadium is high and rather sharp. At 250 Oe the maximum C/T is about $47 \text{ mJ mole}^{-1} \text{ deg}^{-2}$. As the field is increased, the height of the peak decreases and disappears altogether at a field of 1150 Oe. At this field the specific-heat curve has only a rapid change in slope at $T^2 = 3.5 (\text{°K})^2$ in place of the peak.

It has been questioned whether this transition from the superconducting to the mixed state is of first^{20,21} or

second²¹⁻²³ order. High-resolution magnetization measurements on niobium²³ suggest a λ -type second-order transition. To examine this question for vanadium the sample was cooled in zero field, and then a field of 40 Oe was applied. Thereafter the sample was slowly heated and allowed to drift through the transition. No latent heat was observed; instead, C/T reached a maximum of $48 \text{ mJ mole}^{-1} \text{ deg}^{-2}$ over a temperature interval of about 5 mdeg. This gives qualitative agreement with Goodman's calculations²² that show the transition at H_{c1} should be λ type, which is truncated for samples with a nonzero demagnetizing factor. But, on the other hand, the demagnetizing factor would also cause an ideal first order transition to be broadened and truncated, and because of the fairly large demagnetizing factor for this sample, we were unable to establish whether the ideal transition should be first order or second order.

The temperatures at which the peaks in the specific heat occur (see Fig. 11) do not coincide with $H_{c1}(T)$ (to be discussed later) but occurs at higher temperatures, which agrees with observations on niobium.²¹ This difference may be due to a combination of the following:

FIG. 7. Entropy in different magnetic fields as a function of temperature. The entropy curves were made to join the normal-state curve at the transition temperature for that field. The entropies for $H = 552$, 700, and 937 Oe do not approach zero at $T = 0^\circ\text{K}$; this is a result of internal irreversible heating of the sample during specific-heat measurements in those fields.



²¹ T. McConville and B. Serin, Rev. Mod. Phys. 36, 112 (1964); Phys. Rev. Letters 13, 365 (1964).

²² B. B. Goodman, Phys. Letters 12, 6 (1964).

²³ B. Serin, Phys. Letters 16, 112 (1965).

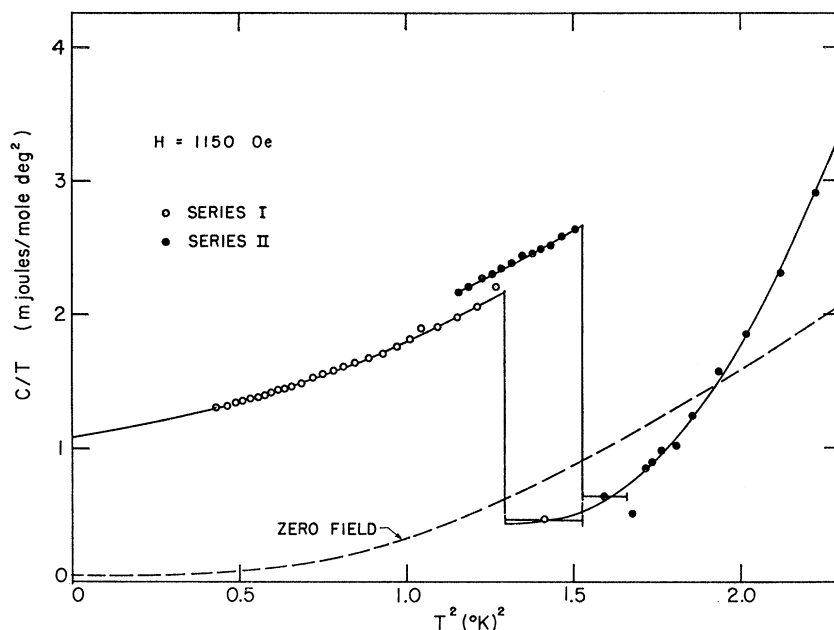


FIG. 8. Anomalous specific heat in a field of 1150 Oe. The series-I data were obtained after cooling in zero field. The series-II data were obtained after cooling from the highest temperature reached in series I. The bars connected to two of the points represent the temperature interval used in measuring the specific heat at each of the two points.

(a) internal heating of the sample as a result of flux jumping at H_{c1} , which lowers the apparent specific heat considerably at H_{c1} but not at temperatures just above this, so that the peak is shifted to a higher temperature, or (b) delayed flux penetration into the sample. Results of entropy calculations are given in Fig. 7 and show that for $H < H_{c1}(0)$ a considerable amount of entropy is missing in all but the lowest field of 250 Oe. In these calculations the mixed state entropy was made to agree with the normal state entropy at the transition from mixed to normal state, and so the missing entropy is seen at low temperatures. In addition, a similar fraction of enthalpy is missing, which means that considerable irreversible internal heating occurs near H_{c1} and tends to suggest that case (a) contributes to the shift in the peak at H_{c1} .

The specific heat in a field of 1150 Oe behaves anomalously at the lowest temperatures as shown in Fig. 6. An enlarged view of this region is given in Fig. 8. Actually, 1150 Oe is just the value of $H_{c1}(0)$, but this measurement is included in the category $H < H_{c1}(0)$ since it had the same initial history, i.e., the field applied after cooling to 1°K in zero field. After cooling from about 1°K to the lowest temperature in the field of 1150 Oe, the measurements of series I were begun. These data as shown in Fig. 8 are definitely higher than the zero-field case at lowest temperatures. This would indicate that some flux has already penetrated the sample, which is to be expected since in this field the effect of the demagnetizing factor and finite temperatures would cause the sample to be in the mixed state, but very near $H_{c1}(T)$. At $T^2 = 1.3(^{\circ}\text{K})^2$ the curve suddenly drops below the zero-field specific heat. The ΔT used for measuring the specific heat at that point is represented in the figure by the bars connected to that point. Following the meas-

urement of the after-drift for this point, the sample was then cooled and the data of series II taken. The fact that these data are slightly higher than those of series I indicates that additional flux has penetrated the sample. The series-II data also drop to an anomalously low value, but not until the temperature just equals the highest temperature reached in series I. Presumably, the anomalously low specific heat is a result of internal heating of the sample due to flux jumping. At higher temperatures, however, the internal heating appears to decrease. Very little heating was observed during the drift periods; thus, nearly all of the internal heating had to occur during the normal external heating period, or in other words, as the temperature of the sample is rapidly increased. Some of the details of the anomalous behavior are not completely understood at this time. The specific heat in a field of 1040 Oe also showed this anomalous behavior but is not displayed in any of the figures.

Figure 9 shows the effect of sample history on the specific heat in a field of 552 Oe. When the sample is cooled into the superconducting state in a magnetic field, some flux is trapped in the sample, as indicated by the higher specific heat at low temperatures and by the absence of the high peak at the transition from superconducting to mixed state. Most important, though, is the fact that just above the transition the specific heat becomes identical to the case of H applied after cooling. This shows that the specific heat in the mixed state above approximately H_c is independent of sample history. It was discussed previously that entropy calculations from specific heat data in fields greater than about $H_c(0)$ gave no indication of internal irreversible heating of the sample in this region. It then follows that the specific heat gives a complete thermodynamic de-

scription of the material in the mixed state above approximately H_c .

C. Specific-Heat Discontinuity at H_{c2}

The discontinuity in C/T at the transition from the mixed to normal states is displayed in Fig. 10. The change of slope in heating and cooling curves also gave approximate values of the specific-heat discontinuity for low fields. The results of cooling curves are not shown in this figure but are about 2-5% less than the results of heating curves. The discrepancy in $\Delta C/T$ determined from specific heat and from heating curves may be a result of a slight rounding of the specific heat just before and after the transition. This rounding was neglected in drawing curves from specific-heat data. This rounding shows up, however, in the heating and cooling curves. Most of the rounding is probably a result of the inhomogeneity of the applied field, and so $\Delta C/T$ from specific heat should be the better curve. This curve was extrapolated to the zero field transition temperature assuming a constant difference in the two curves of Fig. 10. Maki²⁴ showed for alloys that ΔC in the range $T \ll T_c$ can be represented by terms in T^3 and T^5 , which means that ΔC is proportional to T^3 only in the limit of $T \rightarrow 0$. For the case of the pure metal vanadium, however, ΔC is proportional to T^3 for all temperatures up to $T = 4.5^\circ\text{K}$, or $t = 0.84$. In dimensionless form this becomes $\Delta C/\gamma T = (1.97 \pm 0.04)t^2$. For $T > 4.5^\circ\text{K}$ (or $H < 600$ Oe) ΔC increases much faster than T^3 , which appears to be a result of the remnants of the mechanism which gives rise to the peak just above $H_{c1}(T)$. As seen in Fig. 6, the specific heat in a field of 250 Oe does not fully recover from the high peak before the transition to the normal state occurs. Since both heating and cooling curves show a considerable deviation of ΔC from cubic behavior near T_c , the deviation must be a history-independent effect

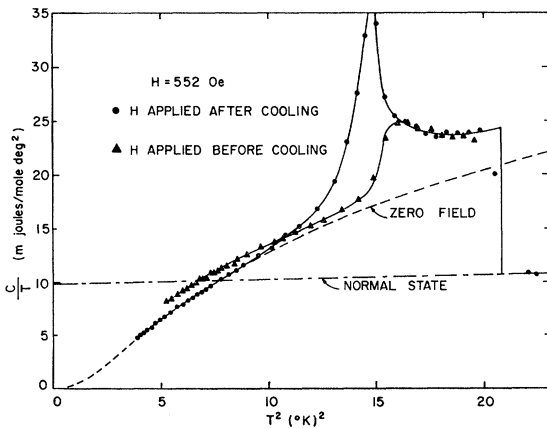


FIG. 9. Specific heat in a field of 552 Oe for the case of H applied after cooling and for the case of H applied before cooling to show the effect of sample history. The maximum C/T is about $39 \text{ mJ mole}^{-1} \text{ deg}^{-2}$.

²⁴ Kazumi Maki, Phys. Rev. 139, A702 (1965).

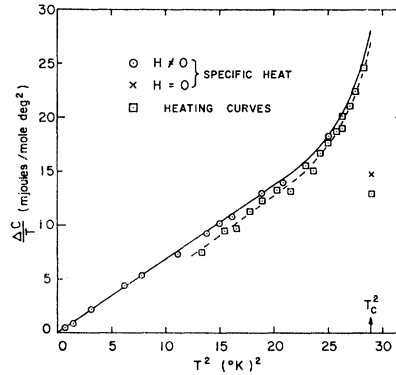


FIG. 10. Jump in specific heat at $H_{c2}(T)$ determined from specific-heat measurements and from heating curves. The solid line was extrapolated to T_c^2 by assuming a constant difference in the two curves. Results of cooling curves are not shown but are 2-5% lower than heating curves.

and not, for example, a result of delayed flux penetration when increasing the temperature. If ΔC_0 represents the jump in specific heat in zero magnetic field, then ΔC does not approach ΔC_0 when T goes to T_c ; see Fig. 10. There is no inconsistency in this condition since ΔC_0 actually represents the difference in specific heats between the superconducting and normal states, whereas ΔC is the difference between the mixed and normal state specific heats. In reality the field was not identically zero, which means that the mixed state was still present in the so called "zero-field" measurements. However, in a field of 0.1 Oe the mixed-state region is less than 1 mdeg wide and gives a negligible energy contribution to specific-heat measurements. Thus, in "zero-field" measurements the specific heat is actually extrapolated through the mixed state from the measurements in the superconducting state, completely neglecting the jump in specific heat between the superconducting and mixed states. Using the theory of second-order phase transitions, Goodman²⁵ showed that

$$\frac{\Delta C}{T} = \left(\frac{\partial M}{\partial H} \right)_{H_{c2}} \left(\frac{dH_{c2}}{dT} \right)^2. \quad (2)$$

For the zero-field transition from the superconducting state to the normal state, the Rutgers relation gives the jump in specific heat as

$$\frac{\Delta C_0}{T_c} = \frac{1}{4\pi} \left(\frac{dH_c}{dT} \right)_{T_c}^2. \quad (3)$$

Dividing the two expressions and letting T approach T_c yields

$$\lim_{T \rightarrow T_c} \frac{\Delta C}{\Delta C_0} = 2\kappa^2 \left(\frac{\partial(4\pi M)}{\partial H} \right)_{H_{c2}, T_c}, \quad (4)$$

²⁵ B. B. Goodman, Phys. Letters 1, 215 (1962).

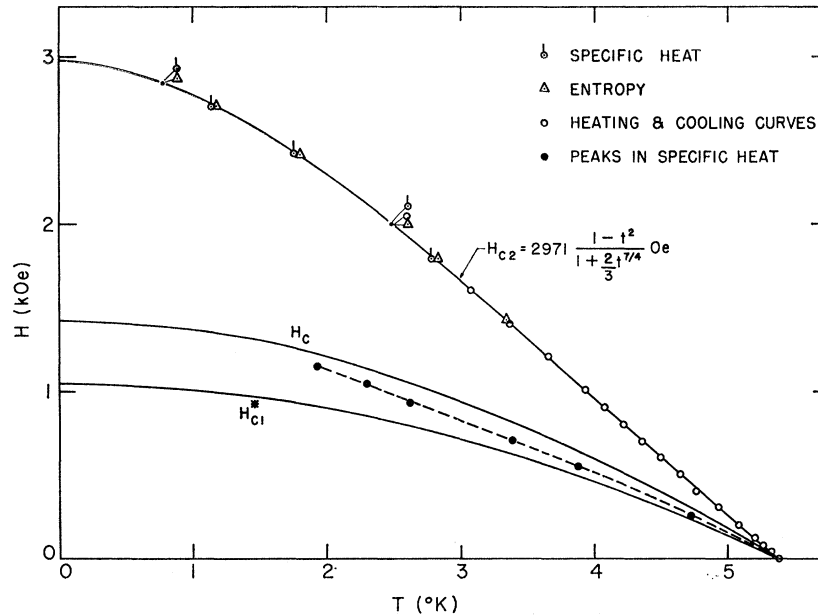


FIG. 11. Critical-field curves for this sample and the position of the peaks in the specific heat. The term $H_{c1}^* = H_{c1}(1-n)$ is the applied field necessary to produce the field H_{c1} in the sample with demagnetizing factor $n=0.092$.

where the Ginzburg-Landau parameter κ is defined as

$$\sqrt{2}\kappa = \lim_{T \rightarrow T_c} \frac{H_{c2}}{H_c} = \left(\frac{dH_{c2}}{dT} \right)_{T_c} / \left(\frac{dH_c}{dT} \right)_{T_c}. \quad (5)$$

The Abrikosov theory¹ of type-II superconductivity, valid near T_c , predicts that

$$\left(\frac{\partial(4\pi M)}{\partial H} \right)_{H_{c2}} = \frac{1}{\beta(2\kappa^2 - 1)}, \quad (6)$$

where β is a constant (1.159 for the more favorable triangular lattice²⁶). Thus, the following equation for $\Delta C/\Delta C_0$ is obtained:

$$\lim_{T \rightarrow T_c} \Delta C/\Delta C_0 = \frac{2\kappa^2}{1.159(2\kappa^2 - 1)}, \quad (7)$$

which is greater than unity for $\kappa < 1.90$. For this sample of vanadium κ equals 0.979 (to be discussed later), so that Eq. (7) becomes 1.76, which is in reasonable agreement with the experimental value of 1.9. Specific-heat measurements²⁷ on the alloy V-5 at. % Ta ($\kappa=7$) show that the ratio $\Delta C/\Delta C_0$ at T_c is less than unity, which is in agreement with Eq. (7).

D. Upper Critical Field $H_{c2}(T)$

Figure 11 shows the upper critical field $H_{c2}(T)$ along with $H_c(T)$ and $H_{c1}^*(T)$. Data for $H_{c2}(T)$ were obtained by finding the transition temperature in several different fields using three methods: (a) heating and cooling

curves, (b) specific heat, using the center of the second-order transition, and (c) entropy curves calculated by assuming zero transition width and deriving the temperature at which the mixed- and normal-state entropies become equal. (In this case we set $S=0$ at $T=0$.) Method (a) was used for fields of 2000 Oe and less and gave especially good results for low fields. Unlike the zero-field case, no supercooling was observed in a magnetic field. Both heating and cooling curves gave the same transition temperature to within experimental error. The experimental error was governed by the width of the transition, which varied from about 0.001°K at 40 Oe to 0.015°K at 2000 Oe. Methods (b) and (c) were used for fields greater than 1400 Oe. The transition width for 2841 Oe was about 0.2°K, so that $H_{c2}(T)$ has the greatest uncertainty in the low-temperature region. As mentioned previously, the inhomogeneity of the applied field was primarily responsible for the transition width. Empirically, $H_{c2}(T)$ is well represented by the rather simple relationship

$$\frac{H_{c2}(t)}{H_{c2}^+(0)} = \frac{1-t^2}{1+\frac{2}{3}t^{7/4}}, \quad (8)$$

with $H_{c2}^+(0) = 2971$ Oe determined from a least-squares fit of the data. The symbol $H_{c2}^+(0)$ is used since it will be shown that $H_{c2}^+(0)$ is slightly higher than the best value of $H_{c2}(0)$. The curve in Fig. 11 is drawn according to Eq. (8). Equation (8) also gives an excellent fit to the niobium data of McConville and Serlin⁷ when using $H_{c2}^+(0) = 3914$ Oe. Deviations from Eq. (8) for vanadium, shown in Fig. 12, at the lower temperatures represent only scatter in the data. For $t \rightarrow 0$ the right side of Eq. (8) becomes $1 - \frac{2}{3}t^{7/4}$, so that $dH_{c2}/dT = 0$

²⁶ W. H. Kleiner, L. M. Roth, and S. H. Autler, Phys. Rev. **133**, A1226 (1964).

²⁷ R. R. Hake, Rev. Mod. Phys. **36**, 124 (1964).

at $t=0$ in accordance with studies on niobium.²⁸ Nevertheless, it seems unlikely that $H_{c2}(t)$ should contain a term of the type $t^{1/4}$ for $t \rightarrow 0$. In fact it will be shown in Subsec. G that the $t^{1/4}$ term gives poor agreement with certain experimental results. For $t < 0.4$ the upper critical field for our sample of vanadium is equally well represented by

$$H_{c2}(t)/H_{c2}(0) = 1 - 1.89t^2 + 0.018t^4, \quad (9)$$

with $H_{c2}(0) = 2960$ Oe. The best value of $H_{c2}(0)$ is then taken as 2960 ± 15 Oe, which is slightly less than $H_{c2}^+(0)$.

For $t > 0.7$ a very small systematic deviation of the data points from Eq. (8) is evident, which amounts to a maximum of about 3 Oe. For $t > 0.85$ the experimental $H_{c2}(t)$ is better expressed as

$$H_{c2}(t)/H_{c2}(0) = a(1-t) + b(1-t)^2, \quad (10)$$

with $a = 1.180 \pm 0.010$, $b = 0.34 \pm 0.02$, and $H_{c2}(0) = 2960$ Oe. Equation (8) leads to the values 1.20 and 0.24 for a and b , respectively, and so represents a good approximation. Strnad and Kim⁸ found that for high-purity niobium, $a = 1.19$, which is nearly identical to that for vanadium. Using the value¹³ $(dH_c/dT)_{T_c} = -469.3 \pm 1.9$ Oe in Eq. (5) leads to the result $\kappa = 0.979 \pm 0.010$ for this sample of vanadium. The error of 0.010 should include both random and systematic errors. The upper critical field as a function of temperature can be expressed in terms of the dimensionless parameter $\kappa_1(t)$ defined by Eq. (1). The experimental behavior of $\kappa_1(t)/\kappa$ is shown in Fig. 13. For this sample $\kappa_1(0)/\kappa = 1.50 \pm 0.02$, which is not much different than the values 1.54, 1.58, and 1.63 (see Refs. 7, 8, 29, respectively) for niobium. In Fig. 13 are also shown various theoretical predictions for $\kappa_1(t)/\kappa$:

Ginzburg³⁰: $\kappa_1(t)/\kappa = 2/(1+t^2), \quad (11)$

Bardeen^{31,32}: $\kappa_1(t)/\kappa = [2/(1+t^2)]^{1/2}, \quad (12)$

Gor'kov³³⁻³⁵: $\kappa_1(t)/\kappa = 1.25 - 0.30t^2 + 0.05t^4. \quad (13)$

The curve of Helfand and Werthamer³⁶ is for the case of infinite mean free path l ; they showed that $\kappa_1(0)/\kappa$ varies from 1.20 to 1.25 as l increases from 0 to ∞ . As

²⁸ G. J. Van den Berg and H. J. M. Van Rongen, *Physica* **30**, 1229 (1964).

²⁹ See Ref. 9. L. Ohtsuka obtained the result $\kappa_1(0)/\kappa = 1.73$ by assuming parabolic behavior for H_c . Using the experimental behavior of H_c [H. A. Leupold and H. A. Boorse, *Phys. Rev.* **134**, A1322 (1964)] yields $\kappa_1(0)/\kappa = 1.63$.

³⁰ V. L. Ginzburg, *Zh. Eksperim. i Teor. Fiz.* **30**, 593 (1956) [English transl.: *Soviet Phys.—JETP* **3**, 621 (1956)].

³¹ J. Bardeen, *Phys. Rev.* **94**, 554 (1954).

³² A. Paskin, M. Strongin, P. P. Craig, and D. G. Schweitzer, *Phys. Rev.* **137**, A1816 (1965).

³³ L. P. Gor'kov, *Zh. Eksperim. i Teor. Fiz.* **37**, 833 (1959) [English transl.: *Soviet Phys.—JETP* **10**, 593 (1960)].

³⁴ Kazumi Maki and Toshio Tsuchiki, *Phys. Rev.* **139**, A868 (1965).

³⁵ L. Tewordt, *Z. Physik* **184**, 319 (1965).

³⁶ E. Helfand and N. R. Werthamer, *Phys. Rev. Letters* **13**, 686 (1964); *Phys. Rev.* **147**, 288 (1966).

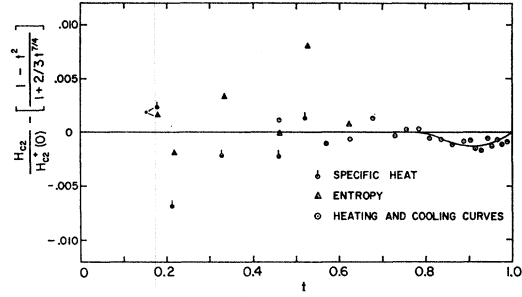


FIG. 12. Deviations of the H_{c2} data from the curve $2971(1-t^2)/(1+\frac{2}{3}t^{1/4})$ Oe.

can be seen, none of the theoretical predictions is satisfactory, but Bardeen's equation has the least deviation from experiment. Both Ginzburg's and Bardeen's equations are, however, phenomenological. Ginzburg made a reasonable choice for the free energy and assumed H_c to have a parabolic temperature dependence. A BCS behavior for H_c would change the value of $\kappa_1(0)/\kappa$ from 2.0 to 1.74, but this still is higher than the experimental findings. The Bardeen equation, which is based on the Gorter-Casimir two-fluid model, has been modified³⁷ to include different coupling strengths. For vanadium the weak-coupling limit is applicable, but than the Bardeen curve should be lowered to $\kappa_1(0)/\kappa = 1.27$, disagreeing further with the experimental results. Both the Gor'kov and the Helfand-Werthamer predictions are based on the GLAG theory and have used the BCS temperature dependence of H_c . Each is a microscopic theory and applicable to the case of pure metals.

Using the GLAG theory, Tewordt³⁵ has shown that the slope of the curve $\kappa_1(t)/\kappa$ versus t at $t=1$ increases monotonically from the value -0.12 to -0.41 as l increases from 0 to ∞ . The slope of -0.41 corresponds to the Gor'kov curve. Experimentally, this limiting

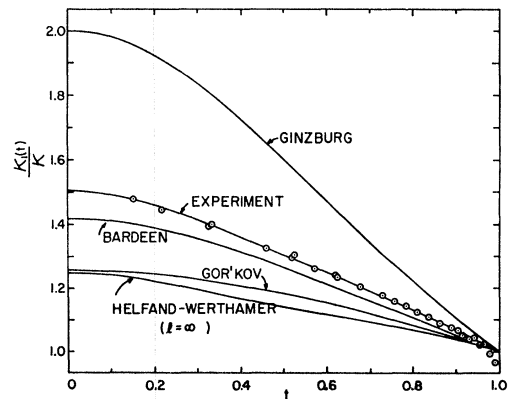


FIG. 13. The temperature dependence of the parameter $\kappa_1(t)/\kappa$, where $\kappa_1(t) = H_{c2}(t)/\sqrt{2}H_c(t)$ and $\kappa = 0.979$ for this sample, compared with several theoretical predictions.

³⁷ A. Paskin, *Phys. Letters* **17**, 235 (1965).

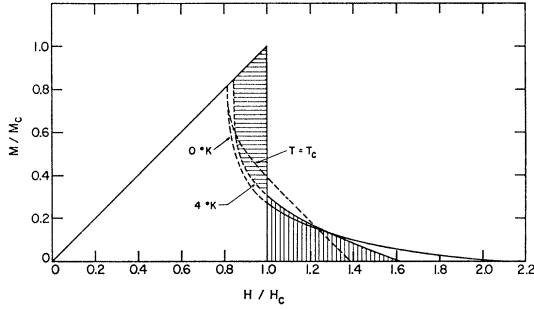


FIG. 14. A reduced plot of the thermodynamically deduced magnetization. For 0 and 4°K the magnetization above $H/H_c=1$ was deduced from specific heat and corrected to zero demagnetizing factor. The curves were extrapolated below $H/H_c=1$ by requiring the horizontally shaded area be equal to the vertically shaded area, as shown for the case of 4°K. The curve for $T=T_c$ is discussed in the text.

slope is given by

$$\left[\frac{d[\kappa_1(t)/\kappa]}{dt} \right]_{t=1} = \frac{ad-bc}{ac}, \quad (14)$$

where a and b are the coefficients in Eq. (10), and c and d are the corresponding coefficients in the expansion of $H_c(t)/H_c(0)$ near $t=1$. For this sample $c=1.777 \pm 0.007$ and $d=-0.593 \pm 0.010$, which, when used with the previously mentioned values for a and b , yield the result -0.63 ± 0.02 for Eq. (14). In most previous investigations of type-II superconductors little attempt has been made to determine the coefficients b and d accurately, and sometimes they have been neglected completely, which leads to incorrect answers for the slope of $\kappa_1(t)/\kappa$ at $t=1$.

E. Thermodynamically Deduced Magnetization and Lower Critical Field H_{c1}

The Gibbs function $G(H,T)$ of the mixed state is found by numerical integration of the relation

$$G(H,T) = G_n(T_H) + \int_T^{T_H} S(H,T) dT, \quad (15)$$

where

$$\begin{aligned} S(H,T) &= S_n(T_H) - \int_T^{T_H} [C(H,T)/T] dT \\ &= \gamma T_H + \frac{1}{3} \alpha T_H^3 - \int_T^{T_H} [C(H,T)/T] dT, \end{aligned} \quad (16)$$

and T_H is the transition temperature in the field H . The Gibbs function of the normal state is given by

$$-G_n(T) = \int_0^T S_n(T) dT = \gamma T^2/2 + \alpha T^4/12, \quad (17)$$

where γ and α are the electronic and lattice specific-heat coefficients. Since history-independent specific

heat is used for the calculation of $G(H,T)$, this function represents a complete thermodynamic description of the material in the mixed state except in the region very near H_{c1} . The magnetization M per unit volume, given by

$$-M(H,T) = (1/V) [\partial G(H,T) / \partial H]_T, \quad (18)$$

(V = molar volume = $8.34 \text{ cm}^3 \text{ mole}^{-1}$) was obtained graphically for $T=0, 1, 2, 3, 4,$ and 4.8°K and then corrected to the case of zero demagnetizing factor, n . Below about H_c , however, magnetization derived in this manner is no longer correct since irreversibilities were present in this region. The correct magnetization in this region between $H_{c1}(T)$ and $H_c(T)$ was found from the equation

$$\begin{aligned} [G_n(T) - G_s(T)]/V &= H_c^2(T)/8\pi \\ &= \int_0^{H_{c2}} M(H,T) dH, \end{aligned} \quad (19)$$

which uses the definition of H_c . In addition, the following assumptions for the case $n=0$ were made: (a) For $H < H_{c1}$ the sample is perfectly diamagnetic, i.e., $-4\pi M = H$ with no rounding at H_{c1} . (b) The slope $\partial M / \partial H$ goes to infinity as H decreases and approaches H_{c1} . The magnetization above H_c was then extrapolated by trial and error to the diamagnetic portion of the curve in such a way that Eq. (19) would hold while meeting condition (b). The thermodynamically deduced magnetization for $T=0^\circ\text{K}$ and 4°K is shown in Fig. 14. The curve for $T=T_c$ is also displayed but will be discussed later. An example of the way in which Eq. (19) was used in extrapolating the curves below H_c is shown in this figure for $T=4^\circ\text{K}$. Equation (19) demands that the horizontally shaded area be equal to the vertically shaded area. Actually assumption (b) is hardly necessary since any reasonable extrapolation under the condition of Eq. (19) requires that the slope be nearly infinite anyway. The point at which the mixed-state magnetization curve meets the diamagnetic portion of the curve is defined as H_{c1} . Whether or not

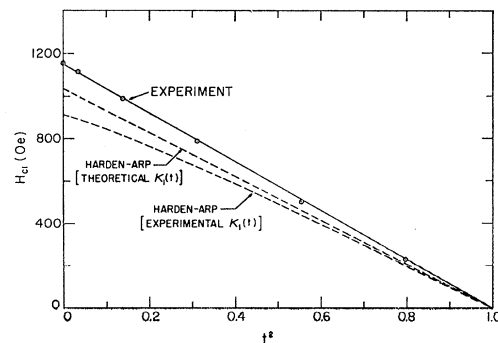


FIG. 15. The temperature dependence of the lower critical field H_{c1} , as determined from the thermodynamically deduced magnetization curves, compared with the prediction of Harden and Arp.

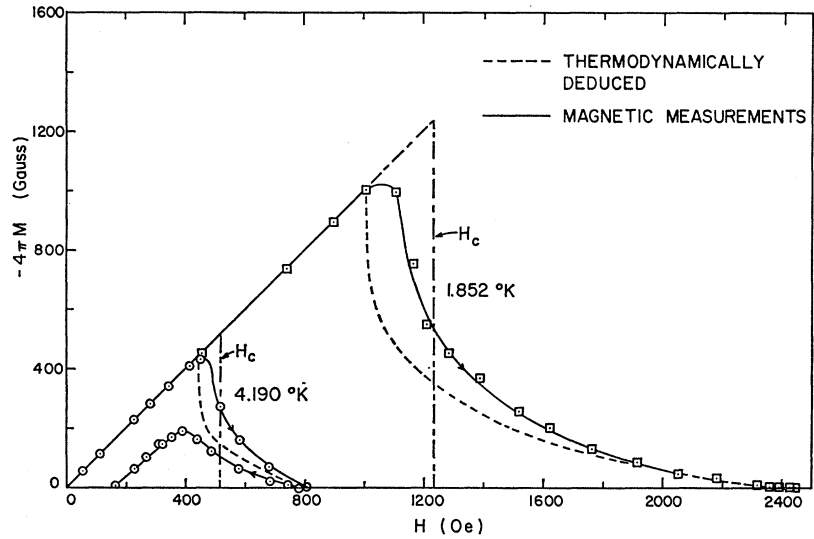


FIG. 16. Comparison of results from magnetization measurements with the thermodynamically deduced magnetization. The curves are corrected to the case of zero demagnetizing factor.

the deduced magnetization above H_c is corrected to $n=0$ makes little difference in H_{c1} obtained in this manner since the resulting fractional change of H_{c1} is about four or five times smaller than the demagnetizing factor. The uncertainty in H_{c1} due to the extrapolation is about 1%, but the uncertainty of the magnetization above H_c contributes an additional 1%.

The magnetization curve for $T=0^\circ\text{K}$ is a very important one since it will be used to obtain certain information about the behavior of the sample at $T=0^\circ\text{K}$. A question, of course, immediately arises concerning the accuracy and reliability of the curve for $T=0^\circ\text{K}$, since some sort of temperature extrapolation is necessary. The magnetization is deduced from the Gibbs function, which in turn is obtained from integration of the entropy according to Eq. (15). Even though extrapolation of the specific heat to $T=0^\circ\text{K}$ is necessary to calculate the entropy at the lowest temperatures, the extrapolation has very little effect on the Gibbs function. Thus, the magnetization curve for $T=0^\circ\text{K}$ should be just as accurate and reliable as the curves for other temperatures.

The magnetic phase diagram of Fig. 11 shows $H_{c1}^* = H_{c1}(1-n)$. The lower critical field H_{c1} for $n=0$, is well represented by the relation

$$H_{c1}(t) = H_{c1}(0)(1-t^2), \quad (20)$$

with $H_{c1}(0) = 1150 \pm 15$ Oe, as shown in Fig. 15. There may be a small departure from parabolic behavior comparable to that for H_c , but the precision of the data is too low to establish this. A parabolic temperature dependence for H_{c1} has been observed in alloys³⁸ and the compound Nb_3Sn .³⁹ In niobium⁶ a slight negative deviation from parabolic behavior appears at low tempera-

tures which amounts to 6% at 0°K . Harden and Arp⁴⁰ have extended Abrikosov's calculation¹ of H_{c1} to the case of small κ , and their calculation in the range $1/\sqrt{2} < \kappa_1(t) < 2$ may be expressed very accurately as

$$H_{c1}(t)/H_c(t) = 0.817[\kappa_1(t)]^{-0.580}. \quad (21)$$

Figure 15 shows two theoretical curves for $H_{c1}(t)$ using for $\kappa_1(t)$ the experimental values and the values predicted by Gor'kov.³³ Both of these curves are less than the experimental $H_{c1}(t)$, but it is interesting to see that nearly a perfect parabolic behavior for $H_{c1}(t)$ is predicted when Gor'kov's values for $\kappa_1(t)$ are used.

F. Magnetization Measurements

The results of the magnetization measurements at two different temperatures, corrected to the case of $n=0$, are shown in Fig. 16. The method of moving the sample between two oppositely wound coils was used for these measurements. The results show a considerable amount of hysteresis, which may be a result of flux pinning at impurity centers and/or critical currents in the surface sheath.⁴¹ Flux penetration begins at the deduced H_{c1} but only very slowly. Extrapolating the mixed-state magnetization curve near H_{c1} , neglecting the rounding, yields values for H_{c1} about 10% higher than the deduced H_{c1} . However, the magnetic measurements give values for H_{c2} that agree with calorimetric determinations. The results for 4.19°K show that for $H > H_c$ the thermodynamically deduced magnetization curve is approximately equal to the average magnetization between increasing and decreasing fields.

Love *et al.*⁴² found for their indium and thallium alloys that by jarring the samples before each measurement, the magnetization above H_{c1} for increasing and

³⁸ W. C. Joiner and R. D. Blaugher, *Rev. Mod. Phys.* **36**, 67 (1964).

³⁹ R. Hecht, *RCA Rev.* **25**, 453 (1964).

⁴⁰ J. L. Harden and V. Arp, *Cryogenics* **3**, 105 (1963).

⁴¹ H. J. Fink, *Phys. Letters* **19**, 364 (1965).

⁴² W. F. Love, E. Callen, and F. C. Nix, *Phys. Rev.* **87**, 844 (1952).

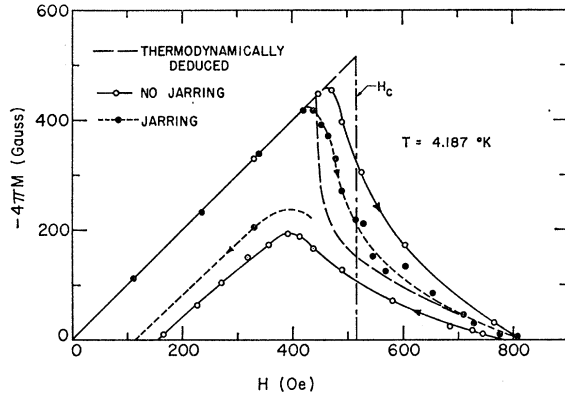


FIG. 17. The effect of sample jarring on the magnetization. The sample was jarred several times before no further change was noticed. The thermal-pulse technique was used for the case of no jarring.

decreasing fields could be made to nearly coincide. Similar results were found for this sample of vanadium. For $H > H_{c1}$ the magnetization in increasing fields was lowered after jarring; it was necessary to jar the sample several times before no further change was noticed. Similarly, for decreasing fields the magnetization increased after jarring. These results are shown in Fig. 17 along with the magnetization measurements with absolutely no jarring. The latter measurements were made by using the heat-pulse technique in which neither coil nor sample is moved, thereby eliminating any source of vibration. As the figure indicates, the hysteresis is greatly reduced by jarring the sample, and the magnetization is in much better agreement with the thermodynamically deduced curve. This supports the contention that specific heat gives a correct thermodynamic description of the material in the equilibrium state. Apparently energy produced by jarring the sample unpins flux lines, so that an equilibrium distribution may be brought about, and also lowers the surface currents which can produce intrinsic hysteresis. Since magnetization showed hysteresis effects, it is surprising to find that the results of specific-heat measurements represent equilibrium behavior for $H > H_c$, because in the latter every precaution was taken to eliminate all sources of vibration.

One further set of magnetization measurements was taken, but this time the sample had the same history as that used in the specific-heat measurements with $H > H_{c1}(0)$, i.e., the sample was cooled to 4.19°K in the applied field for each magnetization measurement. The results for $H > H_{c1}$, however, were still considerably lower than the thermodynamically deduced curve and only about 1.5% higher than for the magnetization where the history was decreasing H at constant T .

G. Evaluation of $\kappa_2(t)$

By using Eq. (2), the limiting slopes $[\partial(4\pi M)/\partial H]_{H_{c2}}$ of the deduced magnetization curves are found from

the jump in specific heat at H_{c2} . This slope as a function of temperature is shown in Fig. 18, and the parameter $\kappa_2(t)$ defined by Maki⁴³ as

$$\left[\frac{\partial(4\pi M)}{\partial H} \right]_{H_{c2}} = \frac{1}{1.159[2\kappa_2^2(t) - 1]} \quad (22)$$

is shown in Fig. 19. Theoretically $\kappa_2(1) = \kappa$ for both clean³⁴ and dirty⁴³ type-II superconductors, so that at $t=1$ Eq. (22) agrees with Abrikosov's prediction [Eq. (6)]. The experimental curves in Figs. 18 and 19 were obtained by using smoothed values of $\Delta C/T$, given by the solid line in Fig. 10. Also included in these figures are points derived from the $\Delta C/T$ data itself to give an indication of experimental scatter. The values of κ_2 and also the temperature dependence derived by Maki and Tsuzuki³⁴ for intrinsic type-II superconductors are in excellent agreement with the observed behavior near the transition temperature. The observed value $\kappa_2(1)/\kappa = 0.985$ is within experimental error of the theoretical value 1.0. Using $[\partial(4\pi M/\partial H)]_{H_{c2}, T_c} = 1.00$ from Fig. 18 and the known value of $(H_{c2}/H_c)_{T_c}$, one can estimate the complete magnetization curve for T approaching T_c if, in addition, the previously discussed conditions on $M(H, T)$ are used. This magnetization is shown in Fig. 14 (labeled $T = T_c$). The value of H_{c1}/H_c obtained from this curve is 0.81 and is smaller than the value 0.911 obtained by using Eq. (20) for $H_{c1}(t)$. This indicates that $H_{c1}(t)$ deviates several percent from parabolic behavior near T_c .

At low temperatures the results $\kappa_2(0)/\kappa = 2.66$ and $[d\kappa_2(t)/dt]_{t=0} = 0$ are found when using in Eqs. (2)

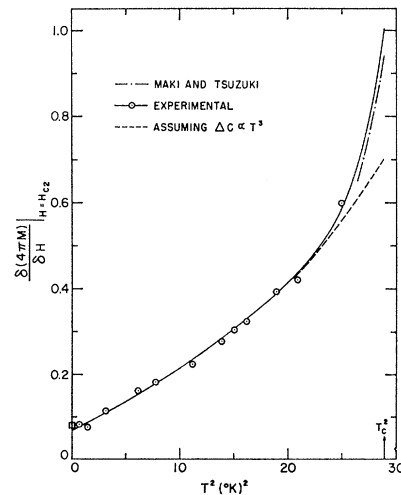


FIG. 18. The slope of the magnetization curves as deduced from the jump in specific heat at H_{c2} . The solid line was obtained by using smoothed values of $\Delta C/T$ from the solid line in Fig. 10. The points are obtained by using $\Delta C/T$ the data itself. The theoretical curve of Maki and Tsuzuki is valid only near T_c . The datum point at 0°K is taken from the slope of the thermodynamically deduced magnetization curve for 0°K.

⁴³ Kazumi Maki, Physics 1, 21 (1964).

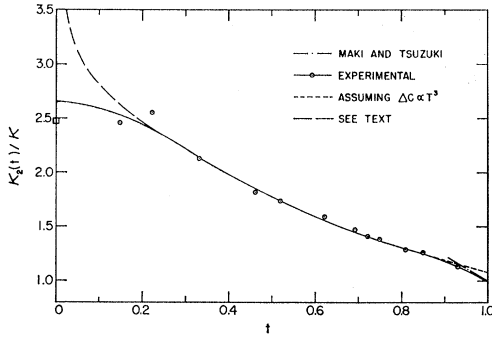


FIG. 19. Temperature dependence of the parameter $\kappa_2(t)/\kappa$ using the data of Fig. 18. The datum point at 0°K , based on the slope of the thermodynamically deduced magnetization curve, is accurate to about 5%.

and (22) the T^3 dependence of ΔC and the equation $H_{c2}(t) = 2960(1 - 1.89t^2)$ Oe for $t \ll 1$. The datum point at 0°K in Figs. 18 and 19 is based on the actual slope of the thermodynamically deduced magnetization curve at 0°K and is accurate to about 5%. Thus, there is no experimental evidence for a divergence of $\kappa_2(t)$ at $t=0$. For a superconductor with no electron scattering Maki and Tsuzuki predict a divergence for $\kappa_2(t)$ at $t=0$ but expect $\kappa_2(0)$ to be finite if scattering is present. The dashed line in Fig. 19 which diverges for low temperatures is the result of using $\Delta C \propto T^3$ and $H_{c2}(t) = 2971(1 - \frac{2}{3}t^{1/4})$ Oe. In addition, any equation for $H_{c2}(t)$ at $t \ll 1$ that contains a term in t of smaller order than two causes $\kappa_2(t)$ to diverge as $t \rightarrow 0$. The fact that these curves do not approach the thermodynamically deduced point at 0°K is a strong indication that $H_{c2}(t)$ should not contain a term in t of smaller order than 2. The theoretical behavior of $\kappa_2(t)$ at intermediate temperatures has not yet been worked out, but Maki and Tsuzuki point out that $\kappa_2(t) \geq \kappa_1(t)$ for all temperatures. In addition they predict that $\kappa_2(t)/\kappa$ for pure metals should be much higher than that of alloys. This is in agreement with our results on vanadium and also with results⁷ on niobium.

H. Calculation of κ_0 , S/S_f , ξ_0 , $\lambda_L(0)$, and l

Gor'kov⁴⁴ derived a general expression for κ valid for both pure metals and alloys: $\kappa = \kappa_0[\chi(\rho)]^{-1}$ where κ_0 depends only on the electronic structure of the metal, independent of electronic scattering. Gor'kov gives an exact expression for the function $\chi(\rho)$ in which $\rho = 0.884\xi_0/l$ with ξ_0 as the BCS coherence length, and l the electron mean free path. The parameter κ_0 may be given by^{4,44}

$$\kappa_0 = 2a\pi\{6/[\zeta(3)]\}^{1/2}\lambda_L(0)/\xi_0 = 0.96\lambda_L(0)/\xi_0, \quad (23)$$

where $a = 0.18$, and $\zeta(3) = 1.202$, and $\lambda_L(0)$ is the London penetration depth. As pointed out by Berlincourt and

⁴⁴ L. P. Gor'kov, Zh. Eksperim. i Teor. Fiz. **37**, 1407 (1959) [English transl.: Soviet Phys.—JETP **10**, 998 (1960)].

Hake,⁴⁵ ξ_0 and $\lambda_L(0)$ can be estimated from the expressions

$$\xi_0 = (akS)/(12\pi T_{c0}\gamma), \quad (24)$$

and

$$\lambda_L(0) = (3h\pi^{1/2}\gamma^{1/2})/(ekS), \quad (25)$$

where S is the area of the Fermi surface in k -space excluding zone boundaries, h is Planck's constant, k is Boltzmann's constant, e is the electronic charge in emu, γ is the electronic specific heat coefficient in ergs $\text{cm}^{-3} \text{deg}^{-2}$, and T_{c0} is the intrinsic transition temperature. Substituting Eqs. (24) and (25) into Eq. (23) yields

$$\kappa_0 = 1.61 \times 10^{24} (T_{c0}\gamma^{3/2}/n^{4/3})(S/S_f)^{-2}, \quad (26)$$

in which n is the number of valence electrons per cm^3 (for vanadium $n = 3.61 \times 10^{23} \text{ cm}^{-3}$) and S_f is the area of the Fermi surface for a free-electron gas of density n .

Goodman⁴⁶ approximated the function $\chi(\rho)$ in such a manner that κ may be expressed as a sum of two terms, viz.,

$$\kappa = \kappa_0 + \kappa_l \quad (27)$$

where κ_l depends on the electron mean free path l . The term κ_l is expressed in terms of measurable quantities as

$$\kappa_l = 7.53 \times 10^3 \gamma^{1/2} \rho_0, \quad (28)$$

where ρ_0 is the normal-state residual resistivity in $\Omega \text{ cm}$. For this sample of vanadium the ratio ρ_{295}/ρ_0 is 140, so that $\rho_0 = 0.143 \times 10^{-6} \Omega \text{ cm}$ when used with the value⁴⁷ $\rho_{295} - \rho_0 = 19.9 \times 10^{-6} \Omega \text{ cm}$. The result $\kappa_l = 0.117$ is then obtained from Eq. (28); a correction⁴⁸ to take into account the small error inherent in the approximation of $\chi(\rho)$ changes the value to $\kappa_l = 0.131$. The experimental value of κ is 0.979, so that κ_0 equals 0.848 ± 0.015 . Since $\kappa_0 > 1/\sqrt{2}$, this result then shows that vanadium is an intrinsic type-II superconductor. The only other element known to be an intrinsic type-II superconductor is niobium ($\kappa_0 = 0.76$).⁶

Tilley *et al.*⁴⁹ found that κ is slightly anisotropic for a single crystal niobium sample, but an approximate average value of κ was obtained with the magnetic field along the $\langle 110 \rangle$ direction. With the field in the $\langle 100 \rangle$ direction κ decreased by about 1.5% from the $\langle 110 \rangle$ direction, whereas in the $\langle 111 \rangle$ direction κ increased by about 1.5%. In this investigation of vanadium the field was along the $\langle 110 \rangle$ direction. Because of the similar electronic and crystal structure, vanadium should also have a slightly anisotropic κ , but the condition $\kappa_0 > 1/\sqrt{2}$ should certainly hold for all directions of the magnetic field.

⁴⁵ T. G. Berlincourt and R. R. Hake, Phys. Rev. **131**, 140 (1963).

⁴⁶ B. B. Goodman, IBM J. Res. Develop. **6**, 63 (1962).

⁴⁷ G. K. White and S. B. Woods, Can. J. Phys. **35**, 892 (1957).

⁴⁸ G. Bon Mardion, B. B. Goodman, and A. Lacaze, J. Phys. Chem. Solids **26**, 1143 (1965).

⁴⁹ D. R. Tilley, G. J. van Gurp, and C. W. Berghout, Phys. Letters **12**, 305 (1964).

TABLE I. Comparison between S/S_f from thermal measurements and anomalous skin-effect (ASE) measurements.

Material	κ_0	S/S_f Eq. (26)	S/S_f ASE
Aluminum	0.0257 ^a	0.61	0.81 ^b -0.99 ^c
Indium	0.112 ^a	0.59	0.60 ^a
Tin	0.164 ^a	0.41	0.44 ^c
Lead	0.38 ^d	0.55	0.54 ^e
Tantalum	0.42 ^f	0.66	
Niobium	0.76 ^g	0.78	
Vanadium	0.848 ^h	0.714	

^a T. E. Faber, Proc. Roy. Soc. (London) **A241**, 531 (1957).

^b R. G. Chambers, Proc. Roy. Soc. (London) **A215**, 481 (1952).

^c T. E. Faber and A. B. Pippard, Proc. Roy. Soc. (London) **A231**, 336 (1955).

^d M. Strongin, A. Paskin, D. G. Schweitzer, O. F. Kammer, and P. P. Craig, Phys. Rev. Letters **12**, 442 (1964).

^e J. E. Aubrey, Phil. Mag. **5**, 1001 (1960).

^f J. Buchanan, G. K. Chang, and B. Serin, J. Phys. Chem. Solids **26**, 1183 (1965).

^g See Ref. 6.

^h This work.

The terms $\lambda_L(0)$ and ξ_0 , as well as the electron mean free path l and the average inverse Fermi velocity $\langle 1/v \rangle_F$, given by⁵⁰

$$l = (6\pi^2\hbar)/(e^2\rho_0S), \quad (29)$$

and

$$\langle 1/v \rangle_F = (6\hbar\gamma)/(k^2S), \quad (30)$$

are all dependent on S . Unfortunately, S has not been measured for vanadium, but it can be obtained from Eq. (26) since all the other quantities are known experimentally. The validity of Eq. (26) is indicated by Table I, where the ratio S/S_f computed for several metals is given and compared with results obtained from anomalous skin-effect measurements. For aluminum, indium, and tin κ_0 was determined from supercooling experiments on high-purity material. Measurements of the surface critical field H_{c3} were used to find κ_0 for lead. For the remaining elements in the table κ_0 was found from measurements of H_{c2} with the aid of Eqs. (27) and (28). The accuracy of S/S_f in both columns of the table for the first four elements is probably not better than about 5%. Except for the case of aluminum, the values for S/S_f determined from Eq. (26) agree remarkably well with the values from anomalous skin-effect measurements. Thus, it appears that thermal or magnetic measurements can be used

TABLE II. Summary of several electronic parameters of pure vanadium.

$\gamma = 1.179 \times 10^4$ erg cm ⁻³ deg ⁻²	$\xi_0 = 450$ Å
$T_{c0} = 5.414$ °K	$l_{\rho_0} = 3.50 \times 10^{-10}$ Ω cm ²
$\kappa_0 = 0.848$	$\langle 1/v \rangle_F = 5.66 \times 10^{-8}$ cm ⁻¹ sec
$S/S_f = 0.714$	$m_i/m = 10.30$
$S = 4.35 \times 10^{17}$ cm ⁻²	$E_F(\text{min}) = 1.47 \times 10^{-12}$ erg (=0.91 eV)
$\lambda_L(0) = 398$ Å	

⁵⁰ E. Fawcett, J. Phys. Chem. Solids **18**, 320 (1961).

quite reliably to find the Fermi surface area of pure superconductors.

According to Eq. (29) the electron mean free path of this sample of vanadium becomes $l = 2450$ Å, which which leads to the result $l/\xi_0 = 5.4$. By Anderson's criterion⁵¹ this sample then is definitely a "clean" superconductor. Table II summarizes the several electronic properties of pure vanadium determined from this investigation. In addition to the quantities just previously defined, this table lists the electronic thermal mass ratio, $m_i/m \equiv \gamma/\gamma_{\text{free}}$, and the minimum value of the Fermi energy, $E_F(\text{min})$. The quantity $E_F(\text{min})$ was calculated from the assumption $\langle v_F \rangle = 1/\langle 1/v \rangle_F$; however, by Schwartz inequality $\langle v_F \rangle$ will be larger than this value for any nonspherical Fermi surface. It was assumed that the intrinsic value of γ would be the same as the γ measured for this sample. Experimentally, the values in Table II are accurate to 2% or better, though considerably larger errors may result from using theoretical equations in the derivation of some of the quantities.

IV. CONCLUSIONS

This work has shown that specific-heat measurements are a powerful tool for determining the behavior of type-II superconductors with small lattice specific heats. The specific heat above H_c , unlike magnetization, is shown to be independent of sample history, and a complete thermodynamic description of the mixed state is derived. In addition, from these measurements the boundaries $H_{c1}(T)$ and $H_{c2}(T)$ of the mixed state are easily established. The thermodynamic critical field H_c is defined unambiguously from specific-heat data in the superconducting and normal states alone. Heating and cooling curves have been used to determine $H_{c2}(T)$ very precisely in the region near T_c , which then has permitted an accurate calculation of κ to be made.

It has been shown that vanadium, like niobium, is an intrinsic type-II superconductor since $\kappa_0 = 0.848 > 1/\sqrt{2}$. The mixed state properties of vanadium are very much like that of niobium ($\kappa_0 = 0.76$), and in particular the parameter $\kappa_1(t)/\kappa$ for this sample of vanadium is nearly identical to that of high-purity niobium. This parameter is about 20 to 50% higher than the corresponding microscopic theoretical predictions³³⁻³⁶ based on the GLAG theory and applicable to pure metals. An improvement is also needed in the prediction of $H_{c1}(T)$. This evidence definitely indicates that the GLAG theory and its extensions to lower temperatures do not give a good quantitative description of intrinsic, low- κ type-II superconductors. It has been suggested⁷ that the discrepancy between theory and experiment may be a result of the failure to include nonlocal electrodynamic effects in the theory. Near T_c the parameter $\kappa_2(t)$, however, is in excellent agreement

⁵¹ P. W. Anderson, J. Phys. Chem. Solids **11**, 26 (1959).

with theory, but at lower temperatures the theoretical behavior of $\kappa_2(t)$ has not yet been worked out. Experimentally, $\kappa_2(t)/\kappa$ for this sample of vanadium is considerably higher than for the case of alloy superconductors,^{7,48} which is in qualitative agreement with theory and with results of niobium.⁷ This work has also shown that calorimetric measurements can be used to give a reliable estimate of the Fermi surface area by

using Eq. (26), which in turn allows accurate calculations to be made for several other electronic parameters.

ACKNOWLEDGMENT

We are grateful to Dr. G. A. Alers of the Ford Scientific Laboratory for loaning us the vanadium sample and for bringing this problem to our attention.

Superconducting Properties of High-Purity Niobium*

D. K. FINNEMORE, T. F. STROMBERG,[†] AND C. A. SWENSON

Institute for Atomic Research and Department of Physics, Iowa State University, Ames, Iowa

(Received 7 March 1966)

Precision magnetization data are given for high-purity niobium metal samples (resistance ratio $R_{300}/R_{4.2}^N = 1600 \pm 400$) over the range from 1.1°K to $T_c = 9.25(\pm 0.01)$ °K. The thermodynamic critical-field curve, which is parabolic to 1%, is that to be expected for an intermediate-coupling superconductor. The magnetization curves are qualitatively like those associated with a type-II superconductor with $\kappa \sim 1$, but the detailed shape does not follow any theory. In particular, the magnetization increases linearly with a slope of 23 G/Oe from 1.005 H_{c1} to 1.025 H_{c1} , where a sharp break occurs to a smaller slope. The magnetization data at H_{c1} and in the region of H_{c2} are consistent with published specific-heat data. The magnitudes of H_{c2} and H_c are consistent with measured values of the penetration depth λ . Preliminary data are reported for H_{c3} as obtained from both resistive and ac susceptibility measurements.

I. INTRODUCTION

THE superconducting properties of transition metals such as niobium, tantalum and vanadium generally have been defined quite poorly when compared with nontransition metals like tin, indium, and mercury.¹ The transition metals were believed to belong to a class of materials (which includes most alloys) which show nonideal irreversible superconducting transitions and considerable irreproducibility from sample to sample.² In contrast, the nontransition metals can be prepared so as to give well-defined and reproducible superconducting transitions. The arbitrariness of this distinction was emphasized when investigations of the superconducting properties of extremely high-purity tantalum^{3,4} metal showed the ideal superconducting behavior which formerly was associated with the softer materials.

Our initial objective was to establish that the superconducting behavior of high-purity niobium metal was similar to that of high-purity tantalum. Our preliminary

results, however, showed quite different types of magnetization curves for equivalent samples (that is, the same resistance ratio and long, thin shape) of the two metals.⁵ For tantalum, complete flux penetration took place over a very narrow region of applied magnetic field, while for niobium the flux penetration was spread over a much wider range of magnetic fields. The magnetization behavior was reversible in both cases, with no locked-in flux. Resistive transition data also suggested a fundamental difference for niobium.⁶ Similar effects have been observed in alloys, and these can be understood in terms of arguments advanced by Pippard⁷ and a theory due to Ginzburg and Landau,⁸ Abrikosov⁹ and Gor'kov¹⁰ (GLAG). These ideas can be discussed in terms of the magnetic field penetration depth λ which is a measure of the depth of penetration of surface currents on a superconducting sample, and the coherence length ξ which is characteristic of the range of order in the superconducting state. As Pippard⁷ has pointed out, the excess surface free energy between

* Work was performed at the Ames Laboratory of the U. S. Atomic Energy Commission. Contribution No. 1753.

[†] Present address: Los Alamos Scientific Laboratory, Los Alamos, New Mexico.

¹ D. Shoenberg, *Superconductivity* (Cambridge University Press, New York, 1952), 2nd ed.

² A. Calverley, K. Mendelssohn, and P. M. Rowell, *Cryogenics* **2**, 26 (1961).

³ D. P. Seraphim, D. T. Novak, and J. I. Budnick, *Acta Met.* **9**, 446 (1961).

⁴ C. H. Hinrichs and C. A. Swenson, *Phys. Rev.* **123**, 1106 (1961).

⁵ T. F. Stromberg and C. A. Swenson, *Phys. Rev. Letters* **9**, 370 (1962).

⁶ S. H. Autler and E. S. Rosenblum, *Phys. Rev. Letters* **9**, 489 (1962).

⁷ A. B. Pippard, *Proc. Cambridge Phil. Soc.* **47**, 617 (1951); *Proc. Roy. Soc. (London)* **A216**, 547 (1953).

⁸ V. L. Ginzburg and L. D. Landau, *Zh. Eksperim. i Teor. Fiz.* **20**, 1064 (1950).

⁹ A. A. Abrikosov, *Zh. Eksperim. i Teor. Fiz.* **32**, 1442 (1957) [English transl.: *Soviet Phys.—JETP* **5**, 1174 (1957)].

¹⁰ L. P. Gor'kov, *Zh. Eksperim. i Teor. Fiz.* **37**, 1407 (1959) [English transl.: *Soviet Phys.—JETP* **10**, 998 (1960)].